Electrochemical and Solid-State Letters, **10** (5) B96-B100 (2007)
1099-0062/2007/10(5)/B96/5/$20.00 © The Electrochemical Society

Mediated Enzyme Electrodes with Combined Micro- and Nanoscale Supports

Scott Calabrese Barton,[a,*,c,z] Yuhao Sun,[a,] Bhupesh Chandra,[b] Sean White,[b] and James Hone[b]**

[a]*Department of Chemical Engineering,* [b]*Department of Mechanical Engineering, Columbia University, New York, New York 10027, USA*

We report the electrochemical performance of a redox polymer-mediated glucose anode catalyzed by glucose oxidase and supported on a multiscale carbon material. The support is composed of carbon paper upon which is grown multiwall nanotubes by chemical vapor deposition combined with ohmic heating of the carbon paper. The material possessed 100-fold higher surface area and demonstrated tenfold higher electrochemical performance, compared to bare carbon paper. Maximum performance is limited by biocatalyst and reactant transport in the micro- and nanoscale pores of the support material.
 [DOI: 10.1149/1.2712049]

Manuscript submitted November 8, 2006; revised manuscript received January 4, 2007. Available electronically March 6, 2007.

The exploitation of ambient fuels is attractive in situations where power needs for small electronic devices are distributed, disconnected, and long-term.[1] This might be true for electronic sensor systems or environmental monitors. Fuel may be derived from carbohydrates contained in plants or from effluent of human or animal processes. Power systems based on ambient fuels will be feasible if the power device itself is capable of generating high electrical power density from plant-derived fuels over long periods. Current biocatalyzed fuel cells are capable of converting such fuels to electricity, but these devices are fundamentally limited by achievable current density, which is orders of magnitude lower than that of precious metal-catalyzed electrodes.

Because of the 5–10 nm size of the typical biocatalyst molecule, sufficiently biocatalytic electrodes tend to be 100 μm to 1 mm in thickness, introducing transport limitations, not only for reactants and products, but for electron transfer to and from the biocatalyst via mediator species.[2] Calabrese Barton and co-workers have employed a carbon paper consisting of ~10 μm diameter carbon fibers with porosity of 78% as the support for an oxygen-reducing electrode catalyzed by laccase. Introduction of the carbon paper support led to a 50-fold increase in electrode surface area and increased oxygen reduction current density by a factor of five[3,4] while maintaining excellent structural properties. A natural extension of this approach is the application of nanotubes on the surface of the carbon fibers. High-porosity carbon paper leads to improved reactant transport and structural stability as compared to carbon black, but the low surface area of carbon papers ($0.16\ m^2/cm^3$) is less desirable as a support material. Application of nanotubes on the surface of the carbon fibers combines the attractive properties of both nanoscale and micrometer-scale materials.[2]

Carbon nanotubes (CNTs) and nanofibers have been applied to electrode materials,[5] catalyst support materials,[6-8] and energy storage,[8-10] due to their unique structural, mechanical, and electrical properties. In the electrodes of a proton exchange membrane fuel cell (PEMFC), carbon black is often used as a support for precious-metal catalysts. The support acts to maintain high dispersion of catalyst nanocrystals while maintaining electronic conductivity. Recent research has demonstrated carbon nanotubes as a candidate material for fuel cell catalyst supports. Carbon nanotubes loaded with Pt and Pt–Ru nanoparticles have shown good electrochemical activity for oxygen reduction and methanol oxidation.[11-15]

Activated carbons which have a large surface area (over $1000\ m^2/g$[16]) may not be suitable for biocatalysts because their micropores are inaccessible, even to electrolyte solution.[17] For example, Barbieri and co-workers compared Brunauer, Emmett, and Teller (BET) surface area to capacitive area of several activated carbons. The capacitive area of Vulcan XC-72 was reported to be $131\ m^2/g$, less than 55% of its BET surface area, $240\ m^2/g$. In addition, the average pore size of wood-based samples, which have a maximum BET surface area, is around 1 nm with almost no distribution above 3 nm, far less than the size of enzyme biocatalysts.[16] Conversely, reticulated vitreous carbon (RVC) possesses high porosity and large pore size but relatively low surface area.[18]

In this paper, a multiscale carbon support material is reported that is produced by growing carbon nanotubes on microscale carbon fibers using chemical vapor deposition (CVD) and ohmic heating.[19,20] Multiwall carbon nanotubes (MWCNTs) were grown on the fibers of carbon paper by ohmically heating iron nanoparticle catalyst sites supported on the carbon fibers. The resulting nanotube growth was visualized by scanning electron microscopy (SEM), and nitrogen physisorption and double-layer capacitance testing provided estimates of overall surface area. Mercury porosimetry was used to study the porosity and pore-size distribution.

The electrochemical performance of the resulting materials was characterized by oxidation of glucose by glucose oxidase coimmobilized with a redox hydrogel mediator within the multiscale carbon structures. The mediator chosen was poly(vinylpyridine)-$[Os(bipyridine)_2Cl]^{+/2+}$,[21] an osmium-based redox polymer with a redox potential of 0.29 V/Ag|AgCl. This high-potential mediator is not ideal for a biofuel cell anode but was chosen to ensure significant catalytic rates, so that biocatalyst loading and mass-transport limitations would be emphasized in electrochemical experiments.

After rendering the multiscale carbon structure hydrophilic by exposure to an air plasma, an aqueous mixture containing the redox polymer, enzyme, and a chemical crosslinker was deposited within the structure and was allowed to crosslink to form a hydrogel. A detailed description of this process is given in Ref. 4. Electrochemical characterization of the resulting structure indicated significantly improved performance, confirming that the current density of biocatalyzed electrodes can be enhanced by increasing the surface area via carbon nanotubes while maintaining high rates of species transport and excellent structural stability via micrometer-scale carbon fibers.

The fabrication process we describe here consists of two deposition steps: nanotube synthesis on the surface of the micrometer-scale support, followed by imbibition of a mediator-enzyme adduct into the resulting structure. The main advantage of the multistep approach is enhanced control of nanotube coverage and morphology without the possibility of harming sensitive bioactive materials. Subsequent functionalization with electroactive materials can be accomplished by various techniques, including imbibition and electrodeposition.[22-24] An alternative approach is to mix a free suspension of nanotubes with enzyme and mediator and to then deposit

* Electrochemical Society Active Member.
** Electrochemical Society Student Member.
[c] Present address: Department of Chemical Engineering and Materials Science, Michigan State University, East Lansing, Michigan 48823, USA.
[z] E-mail: scb@msu.edu

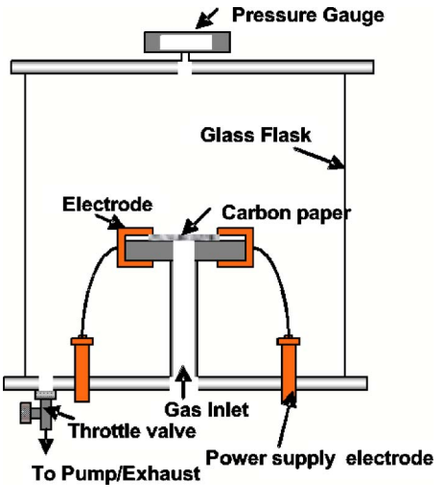

Figure 1. (Color online) Schematic of the nanotube growth system.

this adduct in a single step within the porous support.[25,26] The latter method allows intimate mixing of active material with the carbon nanotubes prior to deposition but is limited in regards to the types of structure that can be achieved afterward. In addition, the choice of final deposition technique is limited to those that do not harm the biocatalyst.

Experimental

Chemicals and materials.— Glucose oxidase (GOx) from *Aspergillus niger* was purchased from Sigma (St. Louis, MO). Carbon paper (Toray TGPH-030, 060, 090 and 120, Japan) was obtained from E-TEK (Somerset, NJ). For comparison purposes, a sample of commercial graphite-modified paper was obtained (GDL 10 AA, SGL Carbon, Charlotte, NC). Ultrapure N_2, He, and liquid nitrogen were purchased from TechAir (White Plains, NY). D-Glucose, sulfuric acid, sodium phosphate, sodium chloride, and sodium periodate were purchased from FisherChemical (Fair Lawn, NJ) and used as provided. Electrochemical measurements were performed in phosphate buffer solution (PBS, 20 mM phosphate-buffered 0.1 M NaCl, pH 7.1). Poly(ethylene glycol) (400) diglycidyl ether (PEGDGE) was purchased from Polysciences (Warrington, PA). The synthesis of redox polymer poly(vinylpyridine), (PVP)-$[Os(bipyridine)_2Cl]^{+/2+}$ was previously reported.[21]

Growth of carbon nanotube electrodes.— Carbon nanotubes were grown directly on carbon paper using a CVD technique.[27,28] In the simplest scheme, a carbon cloth is exposed directly to a solution of iron nanoparticles ($\sim$2 nm diam) in hexane.[29,30] The cloth is then inserted into a CVD reactor and brought to 900°C in a flow of CO mixed with H_2 (1 L/min CO, 1 L/min H_2 in a 1 in. diam quartz tube at ambient pressure); under these conditions, the iron nanoparticles catalyze the growth of single-walled nanotubes. Higher density nanotube growth was achieved by a room-temperature ohmic heating process (Fig. 1).[19,20] In this technique, an electrical current is passed through the carbon paper to heat it, eliminating the need for an external furnace. Furthermore, the CO feedstock was forced to flow through the paper, yielding uniform, controllable growth over a large area. Current was modulated in the 7–8 A range to further improve growth uniformity. This method results in the growth of multiwalled nanotubes with diameters in the $\sim$20 nm range.

Surface area and morphological characterization.— Morphology of the carbon paper before and after deposition of carbon nanotubes was characterized by SEM (Hitachi SEM-4700) at 0.8 kV beam voltage. Surface area was measured by BET nitrogen physisorption[31] using a Gemini 2365 (Micromeritics) as well as the capacitance method described below. Physisorption results were analyzed using the Barrett-Joyner-Halenda (BJH) technique to obtain pore-size distributions in the 2–100 nm range.[32] Porosity and pore-size distribution in the 6 nm to 300 um range were studied via mercury porosimetry using an Autopore 9500 (Micromeritics, Norcross, GA). When possible, measurement repeatability was estimated from measurement of at least three independent samples. Repeatability error is expressed as standard deviation in Table I.

Table I. Material properties of multiscale supports.

Material	Surface area (m^2/cm^3) BET	Surface area (m^2/cm^3) Capacitance[a]	Median pore diameter
Bare carbon paper	0.16 ± 0.02	0.16 ± 0.06	23 μm
Graphite on carbon paper	0.60 ± 0.07	0.69 ± 0.09	30 μm
Nanotubes on carbon paper: Iron catalyzed	9.4 ± 1.4	8.9 ± 1.1	16 nm
Ohmic heated (30 min)	29 ± 4.6	23 ± 2.5	9 nm

[a] Based on a capacitance of 38 $\mu F/cm^2$ calculated from bare carbon paper data.

To obtain sample capacitance, voltammetric curves are recorded in a narrow potential range at varying sweep rates in 1 M sulfuric acid. The current in a nonfaradaic potential range is plotted as a function of sweep rate, the slope of which is the differential capacitance. It is then compared to a reference value C^* to estimate surface area. Because the reference value C^* in sulfuric acid varies from 8 to 45 $\mu F/cm^2$ for various carbon substrates,[33] C^* was calculated such that BET and capacitance-surface-area results were identical for bare carbon paper. The resulting value of C^* was 38 $\mu F/cm^2$.

Enzyme electrodes.— The enzyme composite electrodes were prepared as previously reported.[4] Bare or carbon nanotube-treated carbon cloth was cut into 4 nm diam disks, which were glued to the surface of polished vitreous carbon rotating disk electrodes with conductive carbon paint (SPI, West Chester, PA). The carbon paper was made hydrophilic by exposure to air plasma. The anodic catalyst solution was made as follows: 100 μL of 40 mg/mL GOx in 0.1 M $NaHCO_3$ was oxidized by 50 μL of 7 mg/mL $NaIO_4$ in the dark for 1 h, and then 2 μL of the periodate-oxidized GOx was mixed with 8 μL of 10 mg/mL redox polymer and a 0.5 μL droplet of 2.5 mg/mL PEGDGE. 8 μL of this mixture was pipetted onto the hydrophilic carbon paper. The composite electrodes were cured for $>$18 h in air at room temperature prior to use.

Electrochemical instrumentation.— Electrochemical experiments were carried out in a water-jacketed electrochemical cell containing 80 mL of PBS at 37.5°C. The measurements were performed using a potentiostat (Autolab PGSTAT12). The electrodes were rotated using a Pine Instruments Rotator. The potentials were measured vs Ag|AgCl (3 M NaCl) reference electrode (BAS, West Lafayette, IN). The counter electrode was a platinum wire. When possible, measurement repeatability was estimated from measurements of at least three independent samples. Repeatability error is expressed as error bars representing standard deviation in Fig. 4.

Results and Discussion

SEM morphology.— Figure 2 shows SEM images of carbon fibers comprising the carbon paper substrate with nanotube growth varied by growth time. After only 1 min growth, a "carpet" of short ($<$1 μm) nanotubes appears on the larger carbon fibers. As the growth time increases, the carbon nanotube layer thickens and densifies. After 20 min of growth, the nanotubes begin to significantly fill the void volume between the carbon fibers.

Surface area and pore-size distribution.— Quantitative results of substrate morphology are shown in Table I. Nitrogen physisorption measurements indicate 2 orders of magnitude increase in sur-

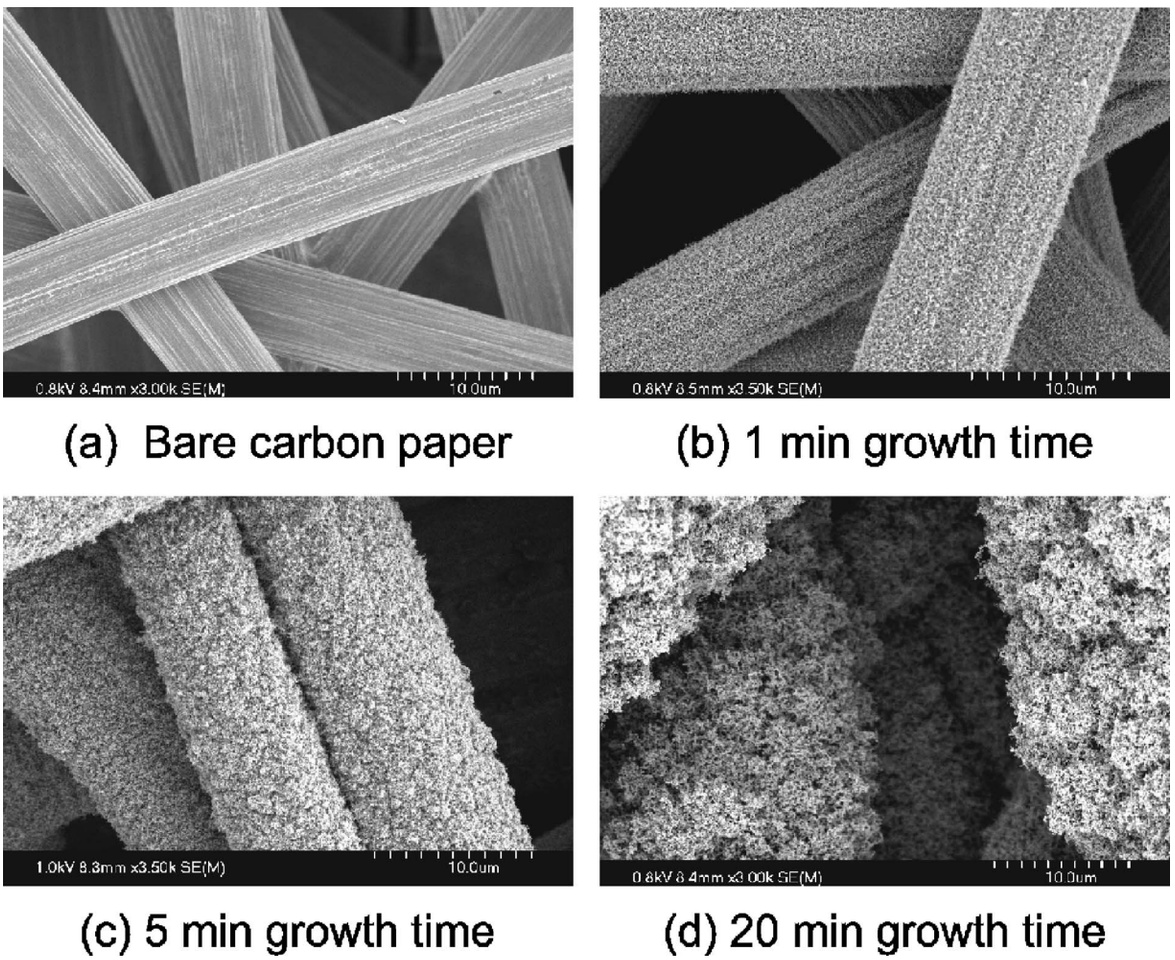

Figure 2. SEM images of ohmic-heated nanotube growth varied by growth time.

face area due to nanotube growth. The surface area is comparable to the results in literature. For example, Wang and co-workers show the surface area of the MWNT-carbon paper composite electrode is in the range between 80 and 140 m^2/g, about the same as the present maximum BET surface area, which is 82 m^2/g, while that of carbon paper alone is less than 2 m^2/g.[34]

Surface area as measured by electrochemical capacitance increased at ~90% of the rate as measured by BET, indicating that ~10% of the area is within pores with length scales that are too small for ionic access. The median pore diameter drops from micrometer to nanometer scales due to nanotube growth.

Figure 3 shows pore-size distributions based on the BJH model. The bare carbon-fiber cloth contains micrometer-scale pores only, whereas nanotube growth introduces nanometer-scale pores. As growth time increased, the nanoscale pore volume increased, indicating higher nanotube density. The peak pore volume with nanotube growth occurs near 17 nm pore diameter, with broad distribution. This range is comparable or slightly larger than the size of the glucose oxidase enzyme (~10 nm).

Anode performance.— Polarization of an electrode catalyzed by glucose oxidase supported on such materials and in the presence of glucose yielded catalytic current that was found to depend strongly on the nature of the carbon support. As measured by maximum catalytic current density, the performance using nanotube-coated carbon-fiber supports increased by up to tenfold over the bare carbon paper, as shown in Fig. 4. To our knowledge, the 22 mA/cm^2 current density reported for GOx immobilized on a multiscale support with 20 min nanotube growth represents the highest current density reported for GOx-catalyzed glucose oxidation. Experimental conditions, including high glucose concentration, high mediator re-

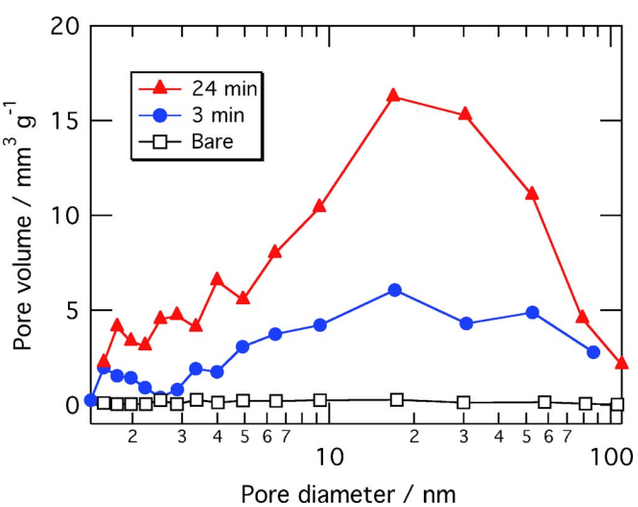

Figure 3. (Color online) Pore-size distribution of multiscale support materials with varying nanotube deposition time.

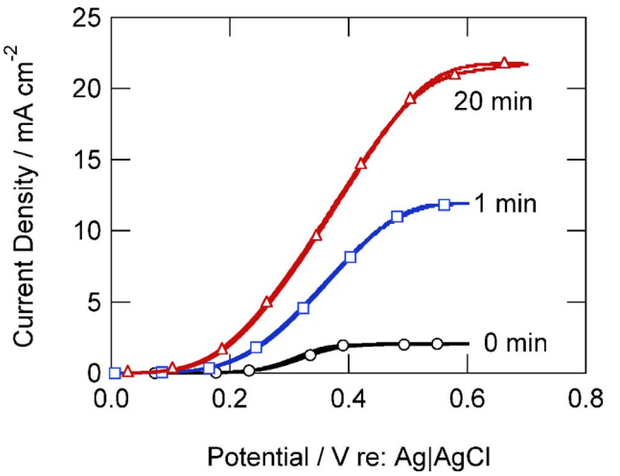

Figure 4. (Color online) Polarization of the glucose oxidase electrodes supported on multiscale carbon supports of 90 μm thickness, varied by nanotube growth time. Nitrogen-saturated, pH 7.1 PBS at 37.5°C, 50 mM glucose, rotating disk electrode at 4000 rpm, −1 mV/s scan rate. Current densities based on 0.13 cm^2 electrodes with 39.6 wt % glucose oxidase, 59.5 wt % mediator, and 0.9 wt % PEGDGE at 0.8 mg/cm^2 total loading.

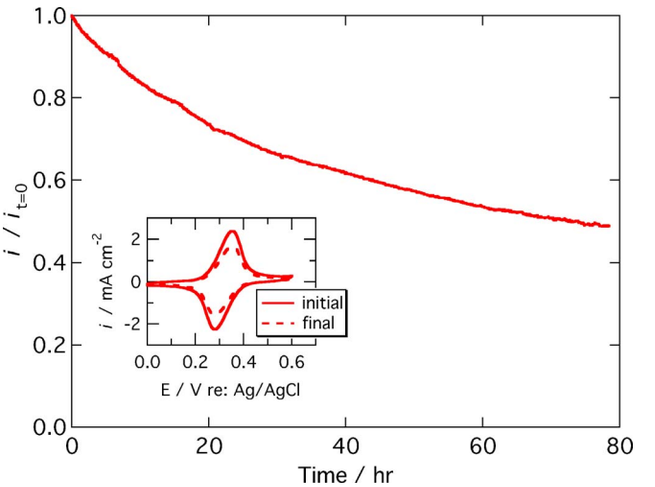

Figure 6. (Color online) Glucose oxidation stability of the multiscale GOx electrode. (a) Time-dependence of the current density of nanotube-treated electrodes poised at 0.5 V re: Ag|AgCl in N_2-saturated PBS (pH 7.1, 37.5°C) with 50 mM glucose, rotating at 1000 rpm. (b) Change in the glucose-free cyclic voltammogram after 80 h operation: 50 mV s^{-1} sweep in N_2-saturated PBS without glucose, 1000 rpm rotation speed.

dox potential, and high disk rotation speed, were chosen to enable such high current density and to highlight the efficient electron transport enabled by the multiscale support. However, the closest current densities reported in the literature for mediated glucose oxidase anodes, mostly obtained under mass-transfer-limited conditions, fall in the 1–2 mA/cm^2 range.[25,35]

These results indicate that electron transfer rates in the glucose anode were increased significantly by implementation of high-surface-area carbon substrates. The increase in catalytic current density does not occur in proportion to increased surface area due to mass-transfer limitations, related to transport of glucose into the porous electrode.[2,36] Additionally, significant surface area within nanopores may not be accessible to the enzyme due either to the size of the enzyme molecule or to high capillary pressure, though 90% of the nanotube surface area is accessible to the electrolyte (Table I and Fig. 5).

Growth time dependence.— Figure 5 demonstrates the effect of nanotube growth time on surface area and electrochemical current density for a 90 μm thick carbon paper substrate. The surface area increased with growth time until about 30 min. However, the observed current densities maximized after only 5 min of growth. Overall, the surface area increased by a factor of 180 and the current density by a factor of 11. This illustrates that increasing surface area is an effective way to improve the performance of an enzyme electrode until the electrochemical process becomes limited by mass transport.

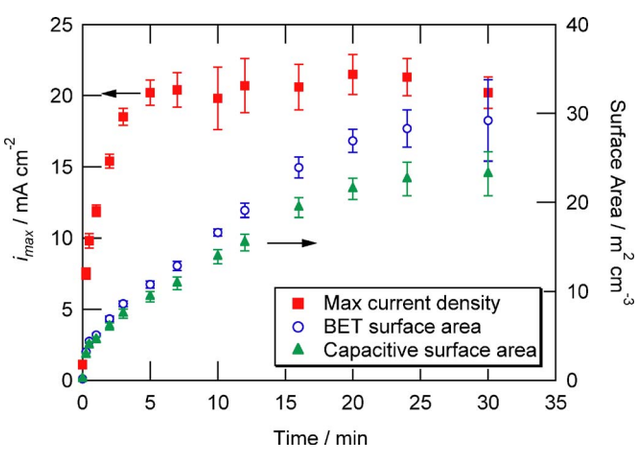

Figure 5. (Color online) Effect of nanotube growth time on surface area and electrochemical current density (conditions as in Fig. 4). Error bars indicate standard deviation for at least three independent samples.

Electrode stability.— The typical half-life of the nanotube-treated electrode was approximately 3 days when poised at 0.5 V vs Ag|AgCl under nitrogen and rotated at 1000 rpm in PBS containing 50 mM glucose, as shown in Fig. 6. The observed loss of activity can be attributed to both enzyme degradation and deactivation of the mediator. The inset to Fig. 6 indicates a ~30% reduction in cyclic voltammetric peak height of the mediator over the course of the 3 day experiment, accounting for just over half of the observed 50% drop in biocatalytic activity. The remainder of the loss may be attributable to reduction in enzyme loading due to leaching in the high-shear environment or to chemical degradation of the enzyme by denaturation or poisoning. These results compare well to the literature,[4,37] indicating that multiscale carbon supports retain the stability of the micrometer-scale carbon-paper-supported electrodes.

Conclusions

High-surface-area carbon materials such as nanotubes immobilized on micrometer-scale carbon-fiber substrates provide an effective way to dramatically improve electron transfer in biocatalytic electrodes without compromising structural strength. Glucose oxidase electrodes have been demonstrated with tenfold improvements in current density due to these multiscale, carbon-based materials. More than 2 orders of magnitude increase in surface area explains this improvement. The ability to fill the void volume of the carbon-fiber paper with conducting nanotubes presents the opportunity to evaluate the performance tradeoff between high-surface-area immobilization and efficient species transport.

Acknowledgment

The authors gratefully acknowledge financial support from the National Science Foundation (Awards CTS-0239013, CHE-0346481, and CMS-0428716). We also thank J. Gallaway for synthesis of the redox polymer, SGL Carbon for providing graphite-

treated carbon paper, and B. Hertzberg and J. Kace for assistance with multiscale support fabrication.

Michigan State University assisted in meeting the publication costs of this article.

References

1. S. C. Barton, J. Gallaway, and P. Atanassov, *Chem. Rev. (Washington, D.C.)*, **104**, 4867 (2004).
2. S. Calabrese Barton, *Electrochim. Acta*, **50**, 2145 (2005).
3. S. Calabrese Barton, H.-H. Kim, G. Binyamin, Y. Zhang, and A. Heller, *J. Am. Chem. Soc.*, **123**, 5802 (2001).
4. S. Calabrese Barton, H.-H. Kim, G. Binyamin, Y. Zhang, and A. Heller, *J. Phys. Chem. B*, **105**, 11917 (2001).
5. M. Endo, Y. A. Kim, T. Hayashi, K. Nishimura, T. Matusita, K. Miyashita, and M. S. Dresselhaus, *Carbon*, **39**, 1287 (2001).
6. R. T. K. Baker, K. Laubernds, A. Wootsch, and Z. Paal, *J. Catal.*, **193**, 165 (2000).
7. C. Park and R. T. K. Baker, *J. Phys. Chem. B*, **102**, 5168 (1998).
8. C. Park, P. E. Anderson, A. Chambers, C. D. Tan, R. Hidalgo, and N. M. Rodriguez, *J. Phys. Chem. B*, **103**, 10572 (1999).
9. G. L. Che, B. B. Lakshmi, E. R. Fisher, and C. R. Martin, *Nature (London)*, **393**, 346 (1998).
10. Y. Y. Fan, B. Liao, M. Liu, Y. L. Wei, M. Q. Lu, and H. M. Cheng, *Carbon*, **37**, 1649 (1999).
11. L. Cao, F. Scheiba, C. Roth, F. Schweiger, C. Cremers, and U. Stimming, *Angew. Chem., Int. Ed.*, **45**, 5315 (2006).
12. L. Li and Y. Xing, *J. Electrochem. Soc.*, **153**, A1823 (2006).
13. B. Rajesh, V. Karthik, S. Karthikeyan, K. R. Thampi, J. M. Bonard, and B. Viswanathan, *Fuel*, **81**, 2177 (2002).
14. G. Girishkumar, K. Vinodgopal, and P. V. Kamat, *J. Phys. Chem. B*, **108**, 19960 (2004).
15. W. Z. Li, C. H. Liang, J. S. Qiu, W. J. Zhou, H. M. Han, Z. B. Wei, G. Q. Sun, and Q. Xin, *Carbon*, **40**, 791 (2002).
16. O. Barbieri, M. Hahn, A. Herzog, and R. Kotz, *Carbon*, **43**, 1303 (2005).
17. J. Chmiola, G. Yushin, R. K. Dash, E. N. Hoffman, J. E. Fischer, M. W. Barsoum, and Y. Gogotsi, *Electrochem. Solid-State Lett.*, **8**, A357 (2005).
18. J. M. Friedrich, C. Ponce-de-Leon, G. W. Reade, and F. C. Walsh, *J. Electroanal. Chem.*, **561**, 203 (2004).
19. P. Smiljanic, T. Dellero, A. Serventi, G. Lebrun, B. L. Stansfield, J. P. Dodelet, M. Trudeau, and S. Desilets, *Chem. Phys. Lett.*, **342**, 503 (2001).
20. X. Sun, B. Stansfield, J. P. Dodelet, and S. Desilets, *Chem. Phys. Lett.*, **363**, 415 (2002).
21. B. A. Gregg and A. Heller, *J. Phys. Chem.*, **95**, 5970 (1991).
22. D. M. Zhou, H. Q. Fang, H. Y. Chen, H. X. Ju, and Y. Wang, *Anal. Chim. Acta*, **329**, 41 (1996).
23. T. Tatsuma, M. Gondaira, and T. Watanabe, *Anal. Chem.*, **64**, 1183 (1992).
24. Z. Gao, G. Binyamin, H.-H. Kim, S. Calabrese Barton, Y. Zhang, and A. Heller, *Angew. Chem., Int. Ed.*, **41**, 810 (2002).
25. M. B. Fischback, J. K. Youn, X. Zhao, P. Wang, H. G. Park, H. N. Chang, J. Kim, and S. Ha, *Electroanalysis*, **18**, 2016 (2006).
26. Y. Yan, W. Zheng, L. Su, and L. Mao, *Adv. Mater. (Weinheim, Ger.)*, **18**, 2639 (2006).
27. S. Zhu, C.-H. Su, S. L. Lehoczky, I. Muntele, and D. Ila, *Diamond Relat. Mater.*, **12**, 1825 (2003).
28. J. Hone, M. C. Llaguno, M. J. Biercuk, A. T. Johnson, B. Batlogg, Z. Benes, and J. E. Fischer, *Appl. Phys. A: Mater. Sci. Process.*, **74**, 339 (2002).
29. Y. Li, J. Liu, Y. Q. Wang, and Z. L. Wang, *Chem. Mater.*, **13**, 1008 (2001).
30. C. L. Cheung, A. Kurtz, H. Park, and C. M. Lieber, *J. Phys. Chem. B*, **106**, 2429 (2002).
31. S. Brunauer, P. H. Emmett, and E. Teller, *J. Am. Chem. Soc.*, **60**, 309 (1938).
32. E. P. Barrett, L. G. Joyner, and P. P. Halenda, *J. Am. Chem. Soc.*, **73**, 373 (1951).
33. K. Kinoshita, *Carbon: Electrochemical and Physicochemical Properties*, Wiley, New York (1988).
34. C. Wang, M. Waje, X. Wang, J. M. Tang, R. C. Haddon, and Y. S. Yan, *Nano Lett.*, **4**, 345 (2004).
35. N. Mano, F. Mao, and A. Heller, *J. Electroanal. Chem.*, **574**, 347 (2005).
36. R. T. Bonnecaze, N. Mano, B. Nam, and A. Heller, *J. Electrochem. Soc.*, **154**, F44 (2007).
37. N. Mano, H. H. Kim, Y. C. Zhang, and A. Heller, *J. Am. Chem. Soc.*, **124**, 6480 (2002).